Available online at www.sciencedirect.com
SCIENCE DIRECT
Tectonophysics 420 (2006) 105–122
TECTONOPHYSICS
www.elsevier.com/locate/tecto

Seismic velocity structure of a large mafic intrusion in the crust of central Denmark from project ESTRID

H. Thybo [a,*], A. Sandrin [a], L. Nielsen [a], H. Lykke-Andersen [b], G.R. Keller [c]

[a] *Geological Institute, University of Copenhagen, Øster Voldgade 10, DK-1350 Copenhagen K, Denmark*
[b] *Department of Earth Sciences, Aarhus University, Finlandsgade 6–8, DK-8200 Aarhus N, Denmark*
[c] *Department of Geological Sciences, University of Texas, El Paso, TX 79968, United States*

Received 2 March 2005; accepted 4 January 2006
Available online 5 May 2006

Abstract

The origin of regional sedimentary basins is being investigated by the ESTRID project (Explosion Seismic Transects around a Rift In Denmark). This project investigates the mechanisms of the formation of wide, regional basins and their interrelation to previous rifting processes in the Danish–Norwegian Basin in the North Sea region. In May 2004 a 143 km long refraction seismic profile was acquired along the strike direction of a suspected major mafic intrusion in the crust in central Denmark. The data confirms the presence of a body with high seismic velocity (>6.5 km/s) extending from a depth of ~ 10–12 km depth into the lower crust. There is a remarkable Moho relief between 27 and 34 km depth along this new along-strike profile as based on ray-tracing modelling of PmP reflections. The lack of PmP reflections at a zone of very high velocity in the lowest crust (7.3–7.5 km/s) suggests a possible location of a feeder channel to the batholith. The presence of volcanic rocks of Carboniferous–Permian age above the intrusion (mafic batholith) suggests a similar age of the intrusion. An older obliquely crossing profile and two new fan profiles deployed perpendicular to the main ESTRID profile, show that the batholith is about 30–40 km wide. The existence of this large mafic batholith supports the hypothesis that the origin of the Danish–Norwegian Basin is related to cooling and contraction after intrusion of large amounts of mafic melts into the crust during the late Carboniferous and early Permian. The data and interpretations from project ESTRID will form the basis for subsidence modelling. Tentatively, we interpret the formation of the Danish–Norwegian Basin as a thermal subsidence basin, which developed after widespread rifting of the region.

Keywords: Mafic intrusion; Batholith; Seismic refraction; Seismic reflection; Basin formation; Thermal subsidence

1. Introduction

The formation of intra-continental sedimentary basins is an enigmatic phenomenon, which may be caused by a variety of tectonic, magmatic and geological processes. There are huge economical interests in understanding the underlying mechanisms, and substantial research has been invested in achieving a better understanding of the tectonic and magmatic processes that govern the formation and evolution of the sedimentary basins. Rift processes in the interior of continents are known to produce deep localised graben structures, which often extend for long distances along their axes. Depending on the fate of these rift structures, they may split continents and lead to the formation of new oceans, such as the Atlantic Ocean. Alternatively, the rifting processes may cease and the resulting, aborted rift structures will remain

* Corresponding author. Tel.: +45 3532 2452; fax: +45 3314 8322.
E-mail address: thybo@geol.ku.dk (H. Thybo).

0040-1951/$ - see front matter © 2006 Elsevier B.V. All rights reserved.
doi:10.1016/j.tecto.2006.01.029

as elongated scars in the upper crust and deeper. Depending on the extent of accompanying magmatism, subsequent thermal contraction of the crust and mantle lithosphere may develop deep, wide depressions, which will be filled with sediments while subsiding, a process that will be further advanced by the subsidence that is caused by the weight of the sedimentary infill.

Recent geophysical research on rift zones has contributed substantially to our understanding of the formation processes. The East African Rift is an example of a presently active rift zone with significant magmatic activity. The Kenya Rift International Seismic Project (KRISP) experiments have shown that the East African Rift Zone in Kenya is underlain by a relatively narrow zone of small seismic velocity in the uppermost mantle interpreted as a zone of partial melt underneath the rift axis (Achauer and Masson, 2002). The top of the crystalline crust contains a series of elongated, localised depressions (grabens), which have been filled with up to 6 km of sedimentary and volcanic rocks (Maguire et al., 1994; Birt et al., 1997) above a slight uplift of the Moho. Stretching models of rift formation predict substantial thinning of the underlying crystalline crust and lithospheric mantle (McKenzie, 1978). However, in central and southern Kenya, the seismically detected crustal thinning is significantly smaller than predicted from manifestations in the upper crust, so other mechanisms must have affected the evolution (Keller et al., 1994). It is possible that the true thinning cannot be measured directly from the present crustal thickness, because magmatic intrusions may have replaced part of the original crystalline crust during the stretching. Thybo et al. (2000) identified seismic reflections, which may be ascribed to magmatic intrusions into the lower crust in Kenya and argue that their presence may mask the true crustal thinning caused by the rifting processes. Recent seismic projects further north along the axis of the East African Rift Zone in Ethiopia have shown the presence of a low-velocity mantle anomaly, which extends deep into the upper mantle and is slightly offset from the main rift axis in central Ethiopia (Bastow et al., 2005; Kendall et al., 2005). The Ethiopian rift zone is highly stretched and is subject to significant magmatic activity. It is therefore surprising that the graben structures in central Ethiopia are relatively shallow and that there is none or only slight uplift of the Moho below the rift valley. Mackenzie et al. (2005) instead find a 10 km thick layer at the base of the crust on the western side of the rift zone, which may represent a layer of magmatic underplating, similar to underplated layers below the Kenya Rift Zone (Hay et al., 1995) and at the margins of oceans (Fowler et al., 1989; Collier et al., 1994; Berndt et al., 2000).

Other rift zones show less magmatic activity. Among the presently active zones, the Baikal Rift Zone in the central part of Eurasia, which is the largest stable continental mass on Earth, probably has produced the smallest amount of volcanic rocks at the surface. There is an ongoing debate if the lithospheric mantle has been thinned in a wide zone around the Baikal Rift (e.g. Gao et al., 1994) or if the mantle has been passively stretched in a narrow, thin, vertical zone, which now can be identified as a narrow low-velocity anomaly in the mantle suture between the Siberian Craton and the surrounding terranes in the Altai–Sayan Fold Belt (Petit et al., 1998).

The North Sea area was rifted in the late Palaeozoic and early Mesozoic. The rifting events created a series of graben structures in the area, including the economically important Central and Viking Graben system (e.g. Ziegler, 1990). Recent research has indicated that some of the graben structures in the whole North Sea area may have formed on top of earlier structures by reactivation of pre-existing faults and weakness zones (Scheck et al., 2002). The graben formation was accompanied by strong magmatic activity, best studied around the Oslo Graben in the northern part of the region. It has been suggested that the wide, Mesozoic to Cenozoic sedimentary basins that cover the North Sea region originated from thermal contraction after the widespread magmatic activity (Sorensen, 1986). This model was substantiated by the interpretation of a large batholith in the crust of central Jutland (Thybo and Schoenharting, 1991) and in Scania at the Danish–Swedish boundary (Thybo, 2001). We use the term batholith for the interpreted large mafic intrusion in the crust. Project ESTRID (Explosion Seismic Transects around a Rift In Denmark) has been designed to study details of the presumed magmatic feature in central Jutland, which is believed to have been emplaced along a transtensional shear zone at its southern edge. This three year project includes acquisition of (1) seismic refraction data along the strike of the crustal body, in order to determine its lateral extent, the significance of magmatic intrusions into the crust and the possible existence of volcanic extrusive rocks in the sedimentary column; (2) a deep seismic reflection profile across the body in order to better constrain the emplacement mechanism and geometry of the intrusions, and (3) a 3D shallow seismic data set to determine if the shear zone is still active. Here, we discuss data from the first subproject, which was carried out in May 2004 with acquisition of a refraction seismic profile along the strike of the presumed batholith (Figs. 1–3). The interpretations show that a high velocity body (6.5–6.8 km/s), which may be interpreted as the batholith, reaches depths of 10–12 km

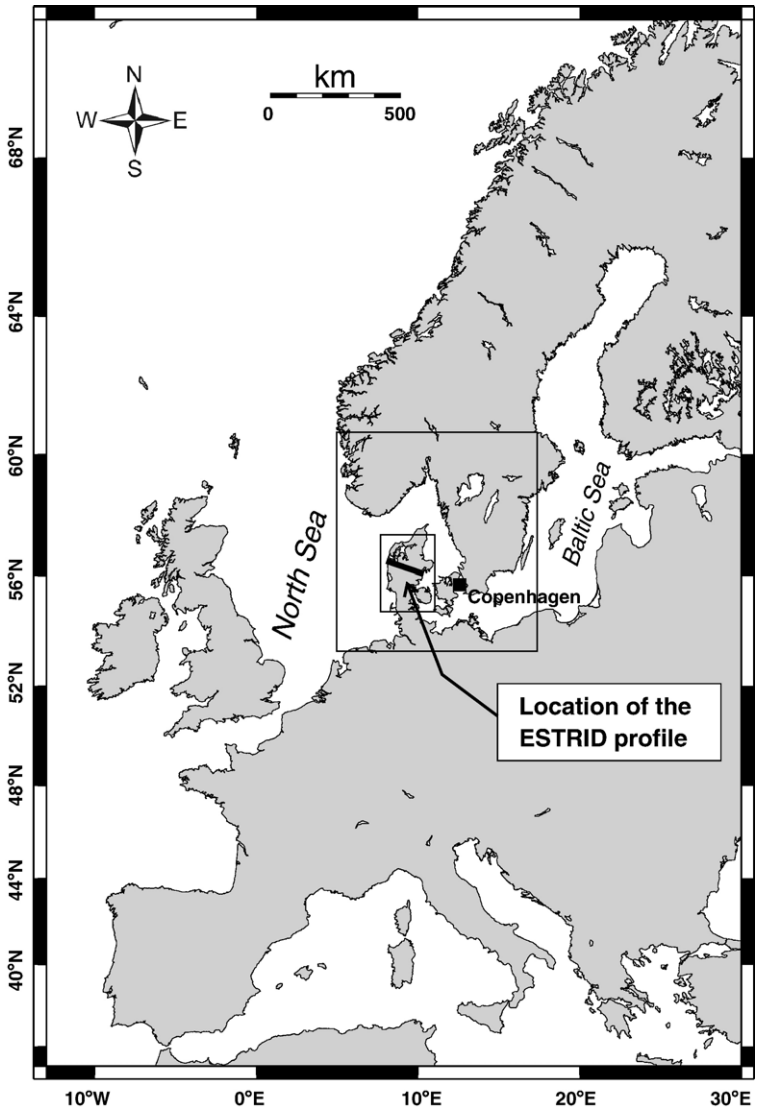

Fig. 1. The location of the ESTRID refraction profiles shown on a geographic map of Europe. The large square shows the extent of the tectonic–geologic map in Fig. 2, and the small square shows the area illustrated in the gravity map in Fig. 3.

in a >80 km long zone. This zone is characterised by surprisingly large variation in Moho reflectivity, which we preliminarily ascribe to remnants of the magmatic processes.

2. Geological–tectonic setting

Oil companies have studied the North Sea region with geophysical methods for decades because of its economical importance. It is generally agreed that the main hydrocarbon bearing structures, the Central and Viking Graben, were stretched by the end of the Palaeozoic and during the Mesozoic (e.g. Ziegler, 1990). Several other graben features developed at the same time throughout Northern Europe (Fig. 2), e.g. the Oslo, Skagerrak, Horn, and Brande Grabens (e.g. Thybo et al., 1990; Vejbaek, 1990; Neumann et al., 1992; Ro and Faleide, 1992). It has been suggested that the extension was due to forces from the Variscan orogeny further south, which caused transtensional movement on the splay of transverse fault zones in the Tornquist Fan (Thybo, 1997). Recent evidence indicates that some of these grabens developed by reactivation of pre-existing graben features (Cartwright, 1990; Abramovitz and Thybo, 2000; Lassen and Thybo, 2004). This regional rifting event was accompanied by substantial magmatic activity (Thybo and Schoenharting, 1991; Neumann et al., 1992; Benek et al., 1996; Thybo, 2001). It has

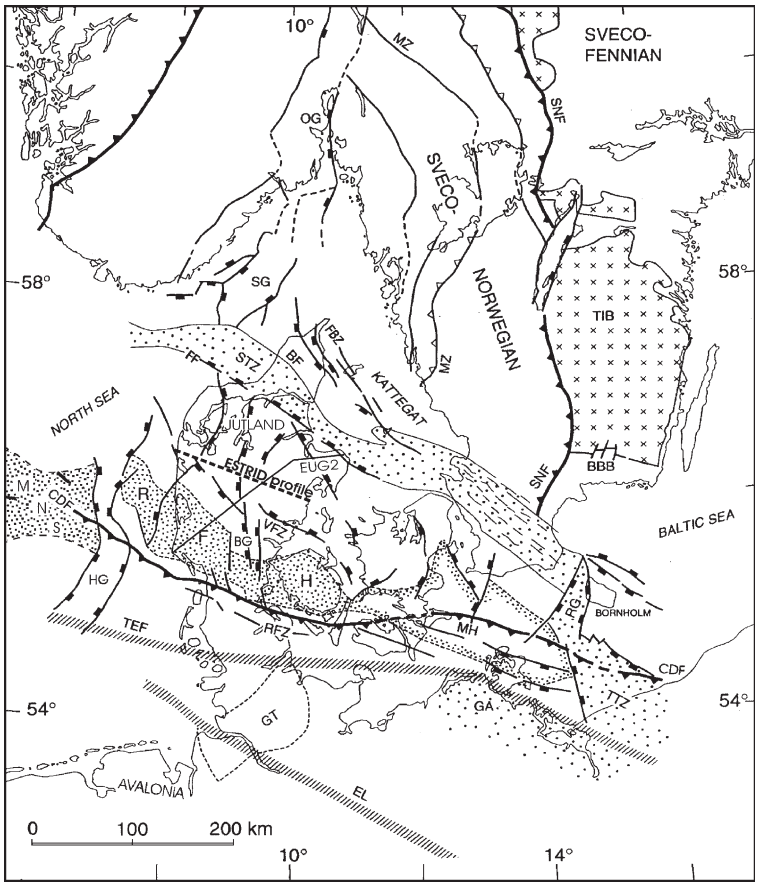

Fig. 2. Map of main tectonic and geologic features of the region around the Danish–Norwegian Basin and the Tornquist Fan region (based on Berthelsen (1992) and Ziegler (1990); after Thybo (1997)). The location of the main ESTRID profile and the EUGENO-S profile 2 (EUG2) are shown in the central part of the map. The Tornquist Fan proper comprises the area between the FBZ and the TEF, incorporating other fault zones such as BF, FF, VFZ and RFZ. Abbreviations: AG — Ålborg Graben, BBB — Blekinge Bornholm Block, BF — Børglum Fault, GB — Brande Graben, BG — Brande Graben, BMF — Bamble Fault, CDF — Caledonian Deformation Front, EL — Elbe Lineament, FBZ — Fennoscandian Border Zone, FF— Fjerritslev Fault, GA — Grimmen Axis, GT — Glückstadt Trough, HG — Horn Graben, MH — Møn High, MNS — Mid North Sea High, MZ — Mylonite Zone, OG — Oslo Graben, RFH — Ringkøbing–Fyn High, RFZ — Rømø Fault Zone, RG — Rønne Graben, SG — Skagerrak Graben, SNF — Sveconorwegian Front, STZ — Sorgenfrei–Tornquist Zone, TEF — Trans-European Fault, TIB — Trans-Scandinavian Igneous Belt, TTZ — Teisseyre–Tornquist Zone, VFZ — Vinding Fault Zone.

been proposed that the uplift caused by the accompanying heating of the lithosphere may have caused strong erosion of the uplifted palaeo-surface, such that the subsequent subsidence due to cooling formed the large and deep regional basins (Sorensen, 1986). This scenario may explain the initial origin of the regional subsidence of the North European Mesozoic basins.

The central part of the Danish–Norwegian Basin includes a characteristic elongated, large positive gravity anomaly of ca. 50 mGal, the Silkeborg Gravity High, in the central part of the Danish–Norwegian Basin (Fig. 3). The characteristic wavelength of the gravity field indicates that the source of this positive gravity anomaly may be located deep in the crust. A previous seismic interpretation along a regional profile across the feature, integrated with gravity interpretation, has indicated the existence of a crustal body with high seismic velocity and density (Fig. 4). The depth to this body is only 10–12 km in its central part over a ca. 55–70 km wide zone, which coincides with the gravity high according to Thybo and Schoenharting (1991). These authors further present seismic, gravity and magnetic evidence for the existence of a layer of volcanic rocks at a depth near the uppermost Palaeozoic strata in the area (6–7 km deep). Reflection seismic profiles indicate ca. 5 km of regional Triassic and Jurassic subsidence, almost without faulting. This evidence may support the hypothesis of a thermal origin of the basin that developed after the rifting processes had ceased.

The earlier geologic history of the region includes Precambrian rifting during the break-up of Rodinia. A recent interpretation of the basement structure of the

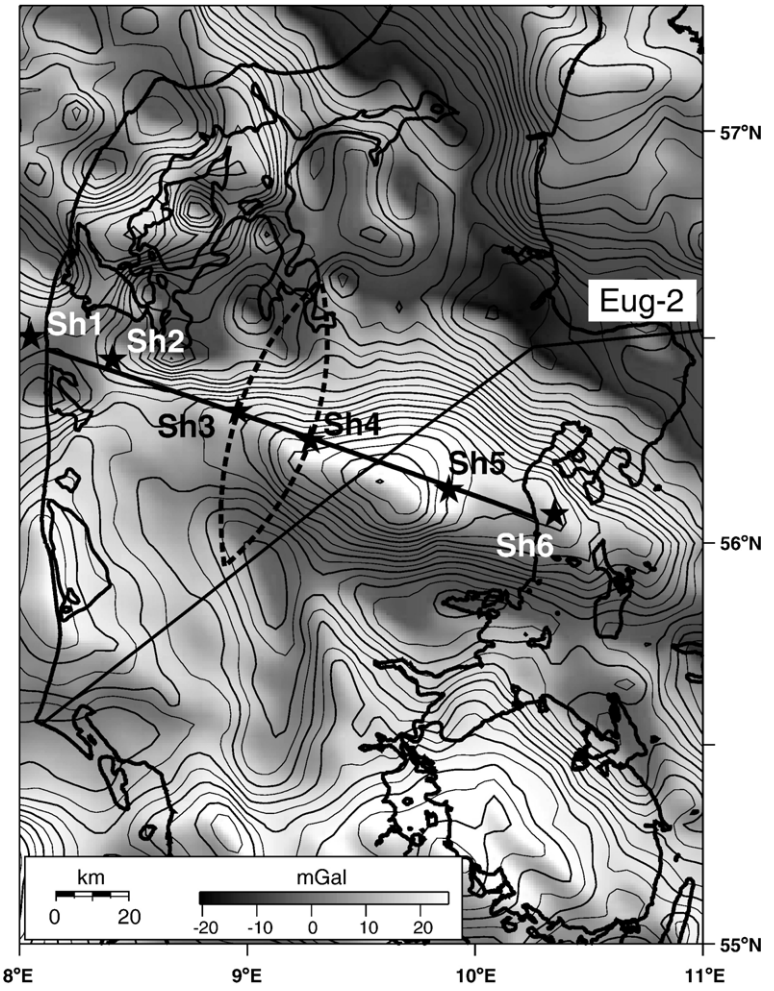

Fig. 3. Maps of the observed Bouguer (onshore) and Free-air (offshore) gravity anomaly field with superimposed locations of the ESTRID profiles and EUGENO-S profile 2 (EUG-2). The gravity data is shown with a grey tone and contours, as well as with shades corresponding to illumination of the gravity relief from the north.

region based on commercial reflection seismic data indicates that this early process may have initiated the faults of the Tornquist Fan (Lassen and Thybo, submitted for publication). The main middle Palaeozoic event was the Caledonian orogeny, when two continents, Laurentia and Baltica collided after closure of the Iapetus Ocean and the exotic microplate Avalonia was amalgamated to the two continents after closure of the Tornquist Ocean. The study area was at that time located at the triple junction between the three plates. Early to middle Palaeozoic sediments were probably deposited and preserved in the foredeeps of the orogens. The structures from these collision events may have influenced the location of the Central and Viking Grabens.

The batholith may have intruded into the crust along a weakness zone caused by the Vinding Fracture Zone, which was first identified from a pronounced linear, magnetic anomaly (Dikkers, 1977). This fault zone is one of the components of the Tornquist Fan and forms the northern edge of the Ringkøbing–Fyn High, which is an east–west trending structural high that separates the northern and southern Zechstein basins (roughly corresponding to the Danish–Norwegian and the North German basins).

3. Seismic data

The seismic data was acquired along an ~ 140 km long profile in May 2004 along the strike of the Silkeborg Gravity High, close to the maximum anomaly, which is about 50 mGal higher than in the surrounding region (Fig. 3). The profile crosses the EUGENO-S refraction profile 2 over the central part of the interpreted batholith in central Denmark (Thybo and Schoenharting,

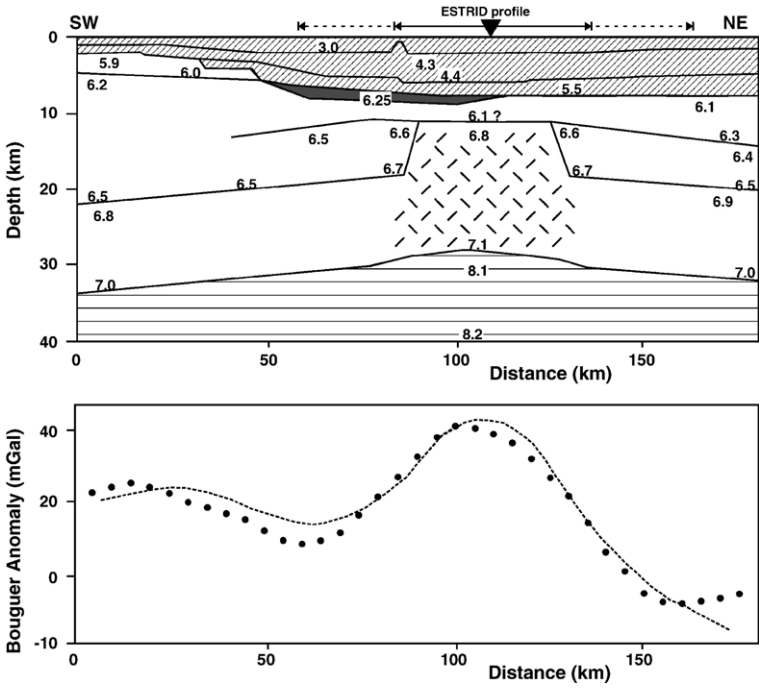

Fig. 4. Seismic velocity model of the crust and uppermost mantle across the Silkeborg Gravity High along EUGENO-S profile 2 (location is shown in Figs. 2 and 3) based on integrated interpretation of seismic reflection and deep refraction, gravity and magnetic data (after Thybo and Schoenharting (1991)). (a) Model of seismic velocity with main tectonic and magmatic features indicated: Interpreted Carboniferous–Permian volcanic body (black) and deep intrusive body (cross hatching), Mesozoic and Palaeozoic sedimentary successions (ruling), upper mantle (horizontal ruling). (b) Gravity fit of the model; the stippled curve shows calculated gravity anomalies and the circles show measured values. The cross point with the ESTRID profile is shown above the profile together with the approximate projected length of the fan profiles (stippled line) and the equivalent reflection points at Moho level (full line) in Fig. 11.

1991). The length of the ESTRID profile was decided by the width of the peninsula, Jutland (Fig. 2), and the wish to identify Pn arrivals from the uppermost mantle. Based on the geometry of the gravity anomaly, we expect the profile to extend along the strike of the central part of the presumed batholith. The purpose of the experiment is to determine the depth to the batholith along the profile, to identify depth variation along the strike of the profile, and to investigate the nature of the magmatic intrusions (e.g. Was the magma emplaced in large magma chambers or in a series of sills? Can possible feeder channels be identified from variation in the wide-angle reflectivity from the lower crust and uppermost mantle?).

Data were acquired with 238 seismographs deployed at 600 m intervals along the central line and 2 times 75 seismographs deployed at 1 km interval along the two arcs across the central line (Fig. 3). All the instruments were Texan 1-component seismographs equipped with 4.5 Hz geophones. The instruments were deployed for the four nights that were required to complete the shooting programme, which suffered from rough weather conditions and technical problems with the two shots at sea. The central line was designed as a traditional seismic refraction and wide-angle reflection profile. The two arcs were designed to provide information about variation in wide-angle reflectivity, including constraints on variation in Moho-depth and in lower crustal reflectivity across the presumed batholith. The two arcs are segments of circles with their centres in the two end shot points, Nos. 1 and 6.

Six shots were detonated to provide the seismic energy. The two offshore shots at the ends of the central profile were detonated at the bottom of the shallow sea at water depths of 12–15 m. Shot point 6 was detonated with 10 individual charges, each consisting of 50 kg of TNT equally distributed along a 100 m long line. Due to rough conditions at sea, shot point 1 was fired with one single charge of 300 kg. Shot point 1 produced a very strong phase (Fig. 5) in the seismic recordings with a velocity of the speed of sound in air (0.33 km/s). This phase is of very short duration, and appears as a usual airwave. However, it was recorded out to offsets of 80–100 km by the geophones, which were all buried to 15–30 cm depth below the surface. Therefore, it is unlikely that this phase propagated in the subsurface between source and receivers. We believe that this wave was propagated as a reflected wave from an atmospheric

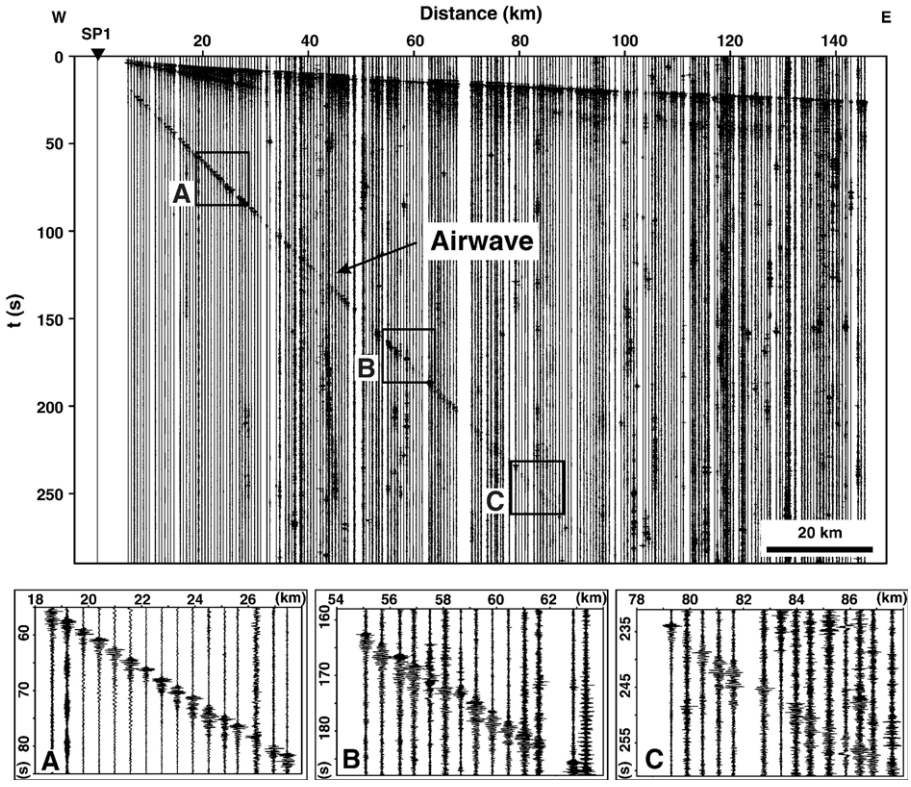

Fig. 5. Seismic section showing a phase with the velocity in air (0.33 km/s) recorded to an offset of almost 100 km from the marine shot point. The seismometers were buried to 15–30 cm depth. Nevertheless, we suggest that the wave has been travelling in the air, probably reflected off a discontinuity in the atmosphere. Three windows (A–C) are shown in detail to illustrate that the waveform is relatively constant along the profile, such that the wave cannot be dispersive and, therefore, not a surface wave.

reflector rather than through the subsurface. Should the wave have been transmitted through the subsurface it would probably have been as a surface wave, but the waveform is not dispersive, which indicates that it must be a body wave in the subsurface or in the air. It is very unlikely that a waveguide with a velocity of 330 m/s can propagate in the subsurface over a more than 80 km long interval, in particular as the other shots in this part of the profile did not excite such waves. An independent indication of the origin of this wave as an airwave was provided by the coast guard in the harbour about 12 km from the detonation point. The explosion he heard was so loud that he became worried of an accident onboard the vessel carrying the charge, so immediately after hearing the detonation, he called the ship over the radio to confirm that the crew was safe. Only few observations are available of such airwaves that propagate over long distances. Similar waves have been observed on a seismic network in the US (Johnston, 1987; Fujita and Sleep, 1991).

The remaining four shots were detonated in 25 m deep boreholes, each loaded with 100 kg of TNT. Shot point 2 had a total charge of 500 kg and shot points 3, 4 and 5 were each charged with a total of 300 kg of TNT. All shots were successful and provided good signal to noise ratio to the farthest seismographs.

All the seismic sections (Fig. 6) show refracted and reflected phases (P_s) with apparent velocities of 1.8–5.4 km/s to relatively large offsets of 20–30 km from the shot points. These phases are followed by a sharp Pg wave of short duration (~ 200 ms) with a velocity of 6.0 km/s in the sections from the westernmost shot points over an up to 20 km long offset interval after which a clear crustal phase with an apparent velocity of ~ 6.5 km/s and larger takes over from offsets of 40–50 km in the west and around 30 km in the east. These high velocities are observed on reversed sections and are therefore close to the true, in situ velocities of the rocks. The high velocity phase is observed to very large offsets, which demonstrates that the corresponding high velocity body extends to deep into the crust. Pn is only observed at the very far end of the section for shot point 1 and possibly on a few traces for shot point 6. This is remarkable as the length of the profile was determined

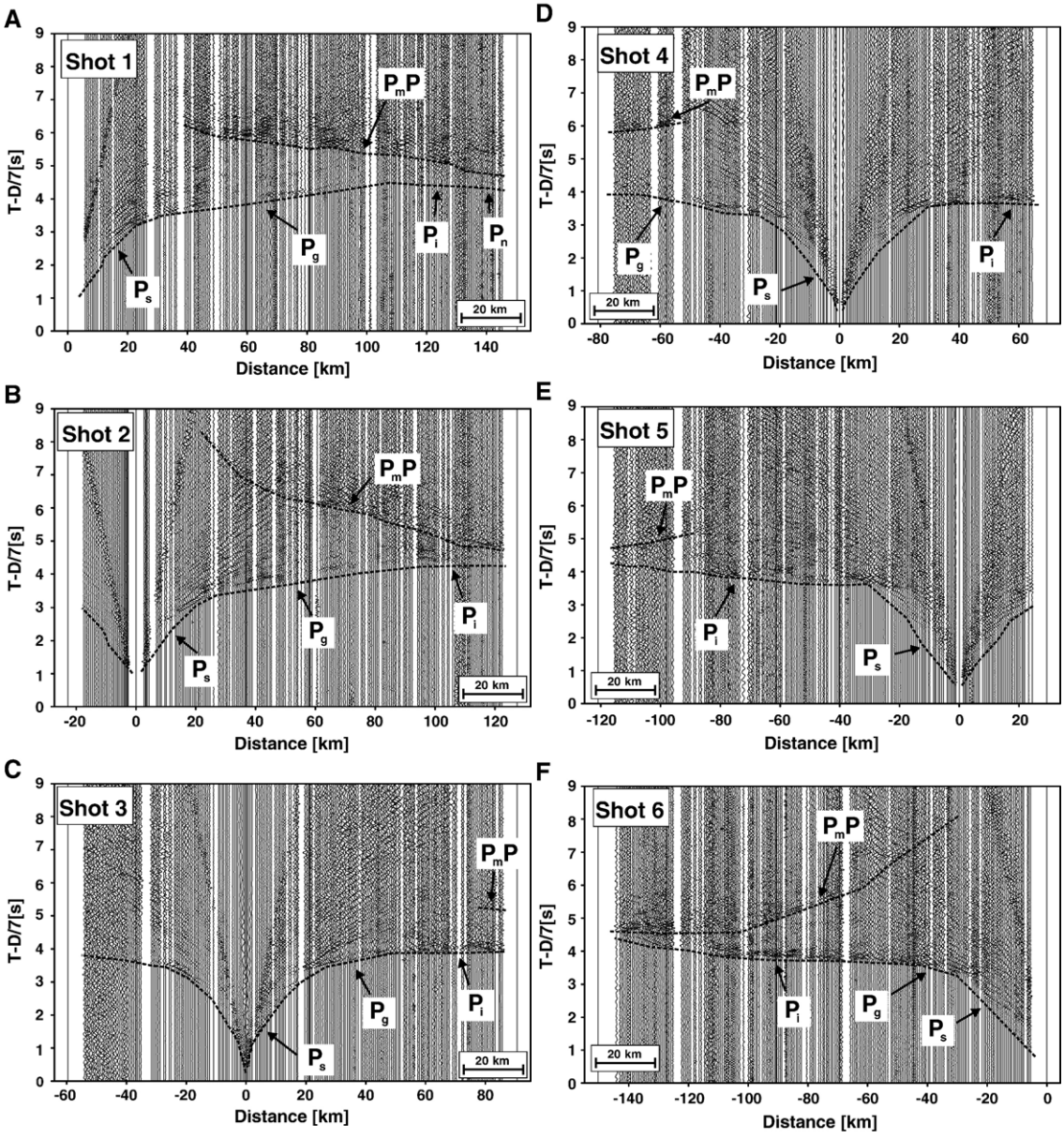

Fig. 6. Seismic record sections recorded along the main ESTRID profile for the six shots. All sections show first arrivals from the sedimentary sequence to offsets of 30–40 km, indicative of a depth to the basement of ca. 10 km. The sections are displayed with a reduction velocity of 7.0 km/s in order to emphasize the very high velocity of the basement in the eastern part of the profile. The Pg has a velocity of ~ 6.2 km/s in the west and the first arrival Pi has very high velocity (>6.7 km/s) to the largest offsets for the recordings in the east. Notice also how the Pi for the eastern shot points 5 and 6 has very high velocity to ca. 40 km from the western end of the recording line, where the velocity drops to ca. 6.2 km/s. These observations clearly demonstrate the extremely high crustal velocity below ca. 10 km depth. The PmP reflection is highly variable along the profile, and even absent in the sections for shot point 3 and 4 recorded towards the east. The PmP is only observed at offsets beyond 90 km in the section for shot point 5. These observations suggest the existence of a 20–30 km wide interval along the profile where the crust–mantle boundary is non-reflective.

to show 20–30 km of Pn arrivals on the sections for the two end shots, based on previous experience from the area. The missing Pn arrivals must therefore be ascribed to the extremely high, mid- to lower crustal velocities in this strike profile over a large depth range, which pushes the cross-over point between crustal and mantle refractions to offsets of more than 125 km.

There are no clear intra-crustal reflections observed in the sections, apart from the short reflections from the sedimentary sequences and a clear reflection from the

top of the crystalline crust in most of the sections. Clear PmP reflections from the Moho are observed on all sections, except for shot points 3 and 4 towards the east. However, the critical offset varies substantially along the profile. This significant variation in Moho reflectivity may be caused by variation in velocity around the Moho in the lower crust and uppermost mantle, as well as by variation in the thickness of the Moho transition. A strong PmP reflection is observed in the section for shot point 1 from offsets of ca. 40 km. The apparent velocity of this reflection at short offset is, however, small which may suggest that its short offset part originates from the lower crust and not from the crust–mantle boundary. The critical offset for shot point 2 is around 60 km and the signal character is reverberant for 1–2 s for both of these two western shot points, at the same locations where the first arrival is sharp with a duration of ~ 200 ms. The sections for shot points 3 and 4 (recorded eastwards) show no PmP reflections. All the eastern shot points, recorded towards the west, show a PmP with a

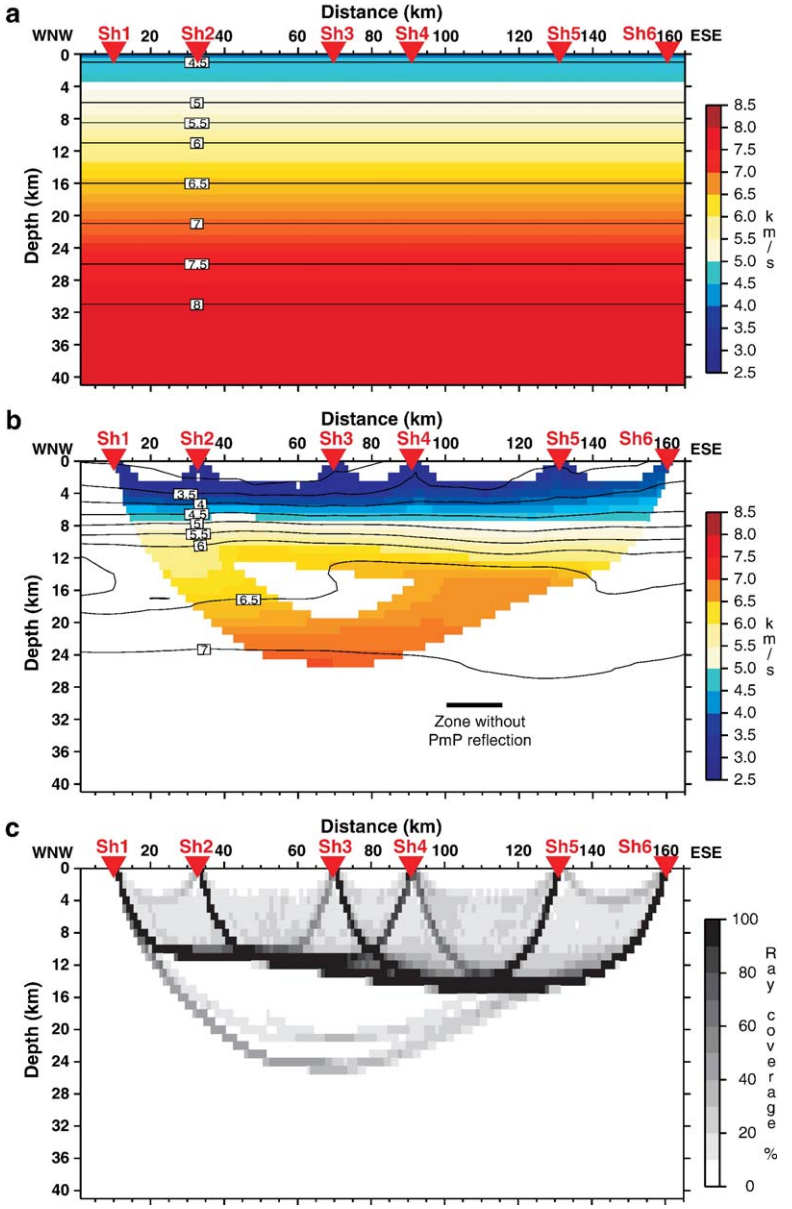

Fig. 7. Model of seismic velocity along the main ESTRID profile, calculated by tomographic inversion of seismic first arrivals. (a) Initial model for the inversion; (b) the final velocity model with a rms-residual time of 89 ms, white parts of the profile are outside ray coverage; the approximate location of the zone without PmP reflections from the crust–mantle boundary is marked; (c) ray coverage in the final model.

compact waveform and with highly variable critical offset: 50 km for SP4 (westward), 90 km for SP5 and 70 km for SP6. Remarkably, the section for SP6 shows no indication for a Pn wave even though the arrival times of the PmP and the Pg waves suggest that a Pn wave with a velocity of 8.0 km/s should be the first arrival over an interval of at least 20 km in the section.

4. Seismic velocity structure

We have determined the seismic velocity of the crust along the main ESTRID refraction profile by tomographic inversion of the travel times of the first seismic arrivals at each seismograph. The first arrival phases are very clear with a high signal to noise ratio in all six seismic sections, such that the uncertainty of the picked arrival times is small (less than 50 ms at short offset, 75 ms at farther offset). The tomographic modelling was carried out using the programme of Hole (1992), which is based on the finite-difference algorithm for fast forward calculation of travel times of first arrivals by Vidale (1988).

The inversion code applies a recursive algorithm, which is based on back-projection along the seismic rays of the first arrival signal between the source and receiver. In each recursion step the travel times of first arrivals are calculated for the previous model; the starting model was a 1D model estimated from results of previous seismic studies of the area (Fig. 7a). Based on the calculated travel times, derivatives and perturbations are calculated by back-projecting the residuals along the rays between sources and receivers. Because the inversion problem is highly non-linear and non-unique, perturbations and derivatives are smoothed in each iteration step, but the model itself is never subject to smoothing. Limited resolution and non-linear effects of the inversion results are often identified as "streaking" in the model where a velocity anomaly is smeared along isolated ray paths. The algorithm was developed for 3-dimensional travel time inversion, but here it is used in two dimensions along the seismic profile.

The inversion algorithm is based on least squares fitting between observed and calculated travel times. In order to account for the limited resolution, the inversion was carried out as a "double-iterative" procedure in outer and inner iteration sequences. In the outer sequence, the offsets taken into account were successively, stepwise increased. In the inner sequence, the size of smoothing filters applied to derivatives and perturbations was successively, and stepwise, decreased while the selected offset interval was kept fixed. The decrease of smoothing filter size, in 4 steps from 160×20 to 10×4 km, stabilize the inversion by primarily distributing model perturbations over large parts of the model for the large smoothing filters and only introducing steep gradients in the later iterations with small smoothing filters at each of the offset intervals. The model was sampled in a 1×1 km grid size and the maximum offsets taken into account in the successive steps were 40, 80, 120 and 143 km, which is the maximum offset in the record sections. This procedure corresponds to carrying out the interpretation "from top to bottom", which further decreases the influence of non-linear effects and non-uniqueness of the model. The root-mean-square travel time residual for the final model is 89 ms, which corresponds to a chi-square measure of around 1.2. This value was selected as a compromise between travel time fit, model resolution and non-linearity. Because the pronounced reflections from the crust–mantle boundary are not taken into account by the method used, and only a few travel times for refractions from the upper mantle are observed, the crustal thickness could not be determined from the explosion sections by this method.

The final model (Fig. 7) demonstrates the presence of very high velocity (>6.5 km/s) beneath a depth of 10–12 km over a 75 km long interval in the eastern part of the profile. The high velocity extends to large depth, at least to the deepest ray coverage at a depth of 26 km. At the western end of the profile, the high velocities of more than 6.5 km/s are encountered at a depth of around 16 km, which is also unusually shallow for the study area. The highest velocity of 7.0 km/s in the central part of the profile is identified at a depth of 24 km. These model velocities should be regarded as minimum velocities, considering that the final model represents a smoothed version of the velocity distribution along the profile. To depths of ~ 10 km, the final model is characterised by low seismic velocities of less than 6.0 km/s with a high vertical gradient, which is typical for the sedimentary sequences. The contours are almost horizontal, which indicates that the sedimentary sequences are relatively flat, as is already known for the Mesozoic sequence from reflection seismic data.

In order to test the reliability of the final tomographic velocity model, we conducted a resolution test. We do not illustrate a checkerboard test because we find that such tests tend to always reproduce the initial cyclic structure, such that a visual inspection may not provide evidence for an assessment of the real resolution of the model. Instead, we designed a model that is close to our interpretation of the final model. For this model, we calculated synthetic travel times, which we used as input to the same tomographic inversion procedure as for the real data. The resulting theoretical model (Fig. 8) shows that we can reproduce the high velocity structure, except

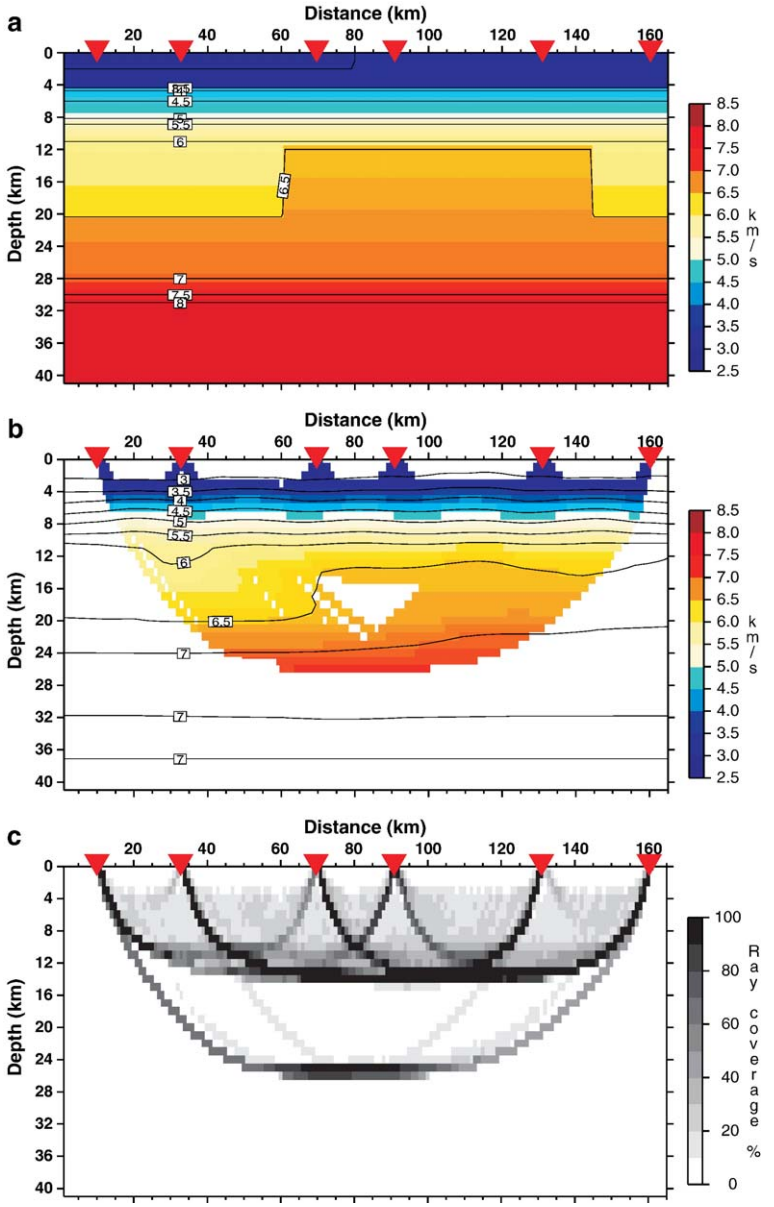

Fig. 8. (a) Theoretical model of seismic velocity, (b) recovered model from inversion of synthetic travel times calculated from the theoretical model, the RMS-residual travel time for this model is 35 ms, and (c) ray coverage in the final model. The similarity between the recovered model and the final model in Fig. 7b indicates the resolution of the method.

for the steepness of the slope on the western side of the high velocity body at around km 65, the size of the zone without ray coverage in the central part of the profile, and the skewness in ray coverage. The sedimentary structure appears well reproduced, and indicates that the depth to the crystalline basement is around 10 km. The result shows further, that the high velocity body must be very shallow (<12 km deep) in most of the eastern half of the profile. The skewness in ray coverage of the final model is not reproduced, but the extremely high velocity of 7.0 km/s at a depth around 20–24 km in the central parts of the profile appears well documented. Experience from testing different theoretical models has further shown that the Moho cannot be much shallower than 30 km along the profile; otherwise we would observe early Pn arrivals in the seismic sections.

The first arrival tomographic model cannot constrain the depth to the Moho, because the Pn wave has only been observed on very few traces. Instead we have interpreted the Moho topography along the profile by ray-tracing

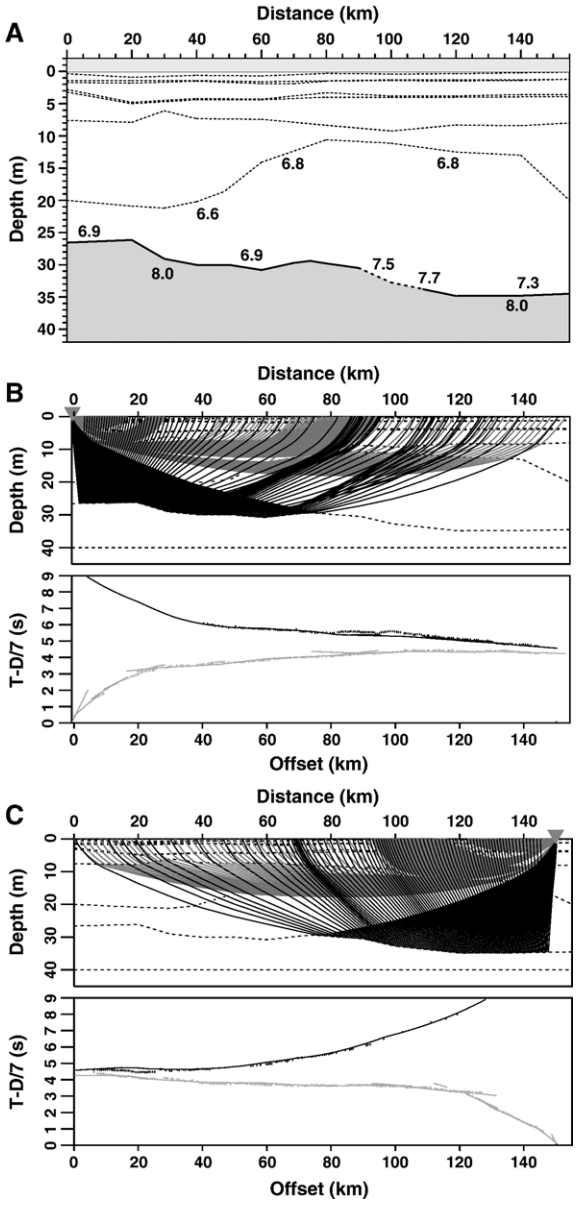

Fig. 9. Ray-tracing result for the ESTRID data. (A) The P-wave velocity model shows strong variation in Moho topography along the profile between 27 and 34 km, which is more than along the cross-profile EUGENO-S No. 2. (B, C) Ray-tracing result for the westernmost shot point No. 1 and the easternmost shot point No. 6, both showing ray traces and calculated travel times superimposed onto a plot of picked arrival times. The model shows significant variation in lower crustal velocity with a variation from 6.9 to 7.5 km/s above Moho, and between 6.6 and 6.9 km/s at the top of the lower crust, depending on the location in relation to the interpreted mafic batholith.

modelling of PmP reflections (Fig. 9). We used the code by Zelt and Smith (1992). There is a surprisingly strong relief on the Moho along the profile between 27 km in the western part and 34 km depth in the eastern part of the profile. Due to the very few observations of the Pn wave, the sub-Moho velocity is assessed to 8.0 km/s with large uncertainty. However, the significant variation in P-wave velocity in the lower crust, just above the Moho, is relatively well constrained. The lower crustal velocity in the high velocity body is 7.3 km/s and significantly higher (7.5–7.7 km/s) in the zone where no PmP reflections has been observed. The very high velocities are encountered in the thick part of the crust along the profile.

The ray-tracing derived model of seismic velocity along EUGENO-S profile 2 (Fig. 4) shows the onset of the 6.8 km/s layer at a depth of 11–12 km, which is comparable to the depth determined along the ESTRID profile. The velocity of the sedimentary sequences is also comparable, taking into account that the ray-tracing model includes more details than the tomographic model. The difference in velocity of the high velocity body between these two models may be ascribed to the stronger smoothing applied to the tomographic model, such that the true seismic velocity at the upper part of the high velocity body presumably is close to 6.8 km/s, also along the strike direction of the body. Future interpretation will focus on the possibility of anisotropy.

5. Lower crustal and Moho reflectivity

The reflectivity from the lower crust and Moho is highly variable along the ESTRID profile, which is only about 140 km long. The absence of PmP reflections in some of the sections corresponds to a non-reflecting Moho in the distance interval of km 85–100 along the profile. The exact location of this interval will be better constrained when the actual topography of the Moho has been modelled with ray-tracing methods. A dipping reflector may change the actual location of the expected reflection points substantially. One may speculate that the lack of PmP reflections is indicative of the location of feeder channels to the inferred batholith. Such feeder channels may be characterised by elevated velocity, and depending on the cooling rate, they may have fairly homogeneous velocity, such that the expected contrast at the Moho level will be seismically invisible. It is definitely unusual not to observe any PmP reflection in this area.

To further illustrate the implications of the variability in PmP reflectivity, we present the results of frequency filtering in three frequency windows of the seismic data (Fig. 10). The zone free of PmP reflections clearly shows no reflectivity in any of the frequency intervals. The section for shot point 1 displays a PmP reflection to very short offset at all frequencies; at high frequencies this reflection is most pronounced and distinct at the

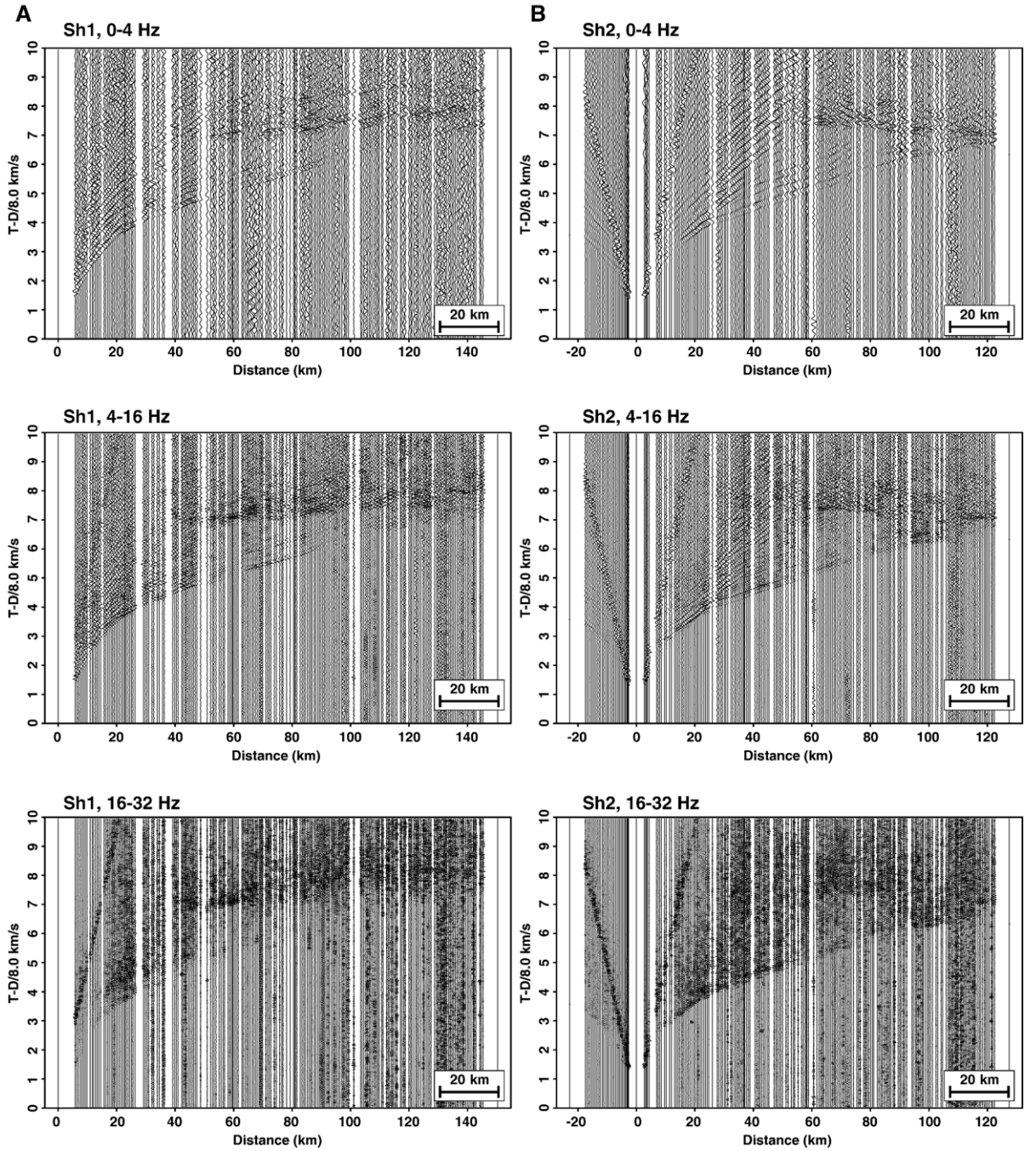

Fig. 10. Results from band pass filtering in three frequency intervals of the seismic data from four of the ESTRID shot points. The filtering illustrates the characteristics of the variable PmP reflectivity from the Moho and the lower crust.

shortest offset. At larger offset the high frequency response is more diffuse, whereas the lower frequency response is distinct and clear. The longest observed waveform is at the high frequencies. The same type of frequency response is found for shot point 2, where however the reverberative character of the reflection is also pronounced at low frequencies and there is a tendency for lower crustal reflectivity in the far offset interval of 80–120 km. The high frequency PmP response is very diffuse, almost to the degree where the signal disappears. The reflection character in the section for shot point 4 to the west is remarkable, as

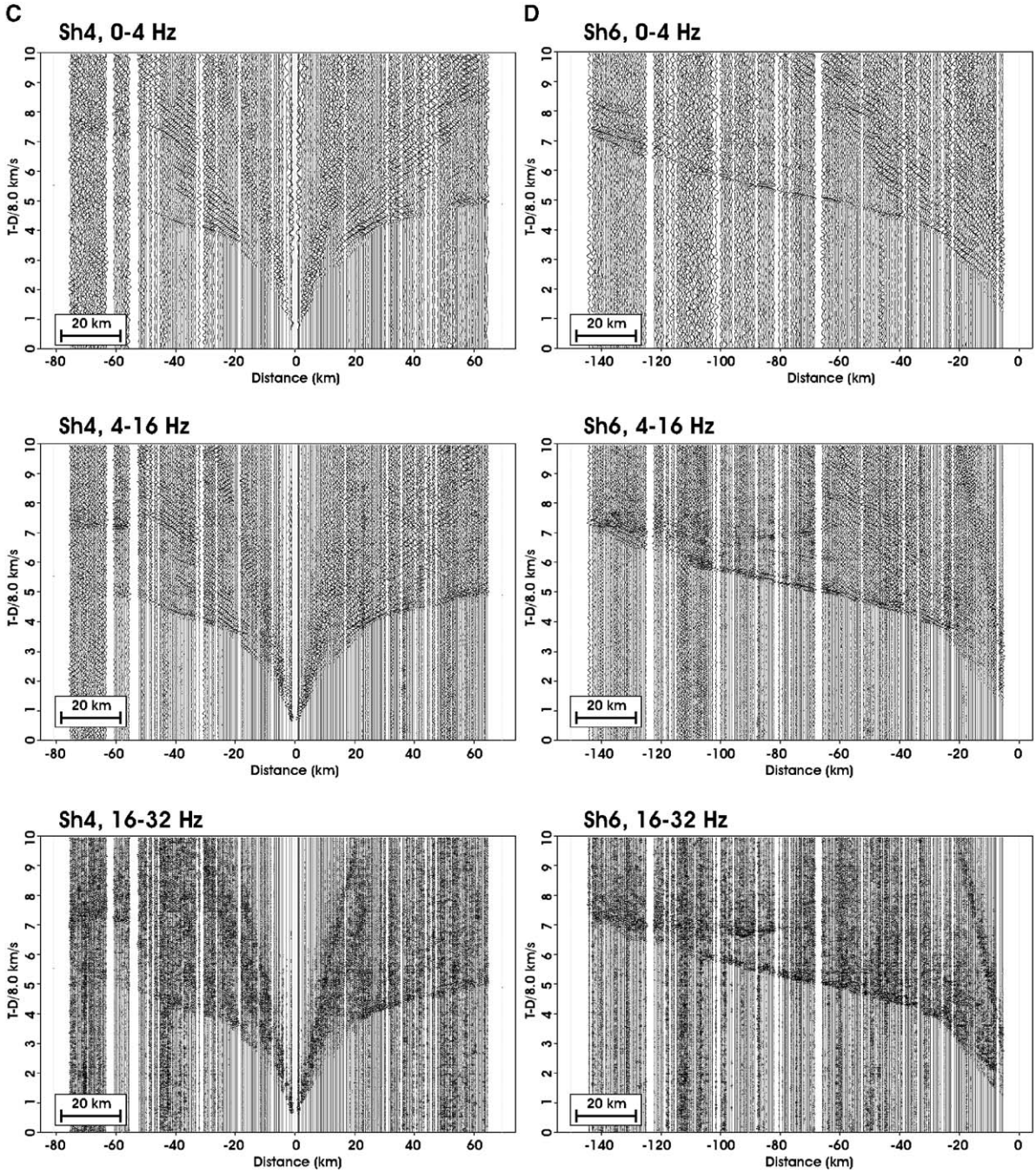

Fig. 10 (*continued*).

there is barely any amplitude at low frequency, but very strong and distinct signal at the high frequencies, indicative of a very abrupt vertical change in velocity at the Moho. A similar observation is made for shot point 6, which also barely shows any PmP at the low frequencies and a strong distinct appearance in the high frequency interval.

Observations on the two sets of fan recordings (Fig. 11) illustrate the variability in reflection character in the lower crust and Moho across the batholith in a direction perpendicular to the main profile. The first onset of seismic energy in these sections corresponds to the direct arrival. The western arc was recorded with reflection points in the same distance range as the interval where

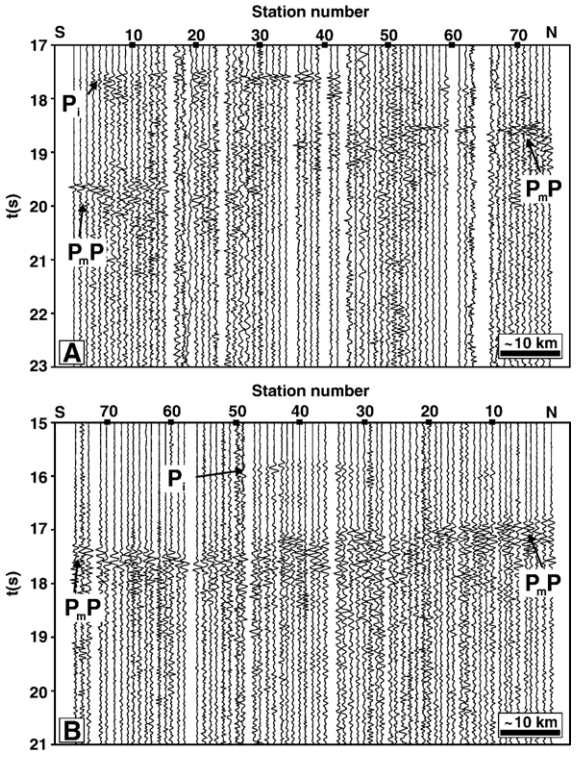

Fig. 11. Seismic sections for the recordings on the two fan profiles: (A) recordings on the western fan of seismic waves from the easternmost shot point 6, i.e. with reflection points in the centre at profile distance km 115 (in the PmP free zone); (B) recordings on the eastern fan of seismic waves from the westernmost shot point 1, i.e. with reflection points in the centre at profile distance km 50. There is strong lateral variability of the reflection response from the Moho: spanning from a reflection free central zone in a), over distinct reflections in the southern end of both profiles, to reverberative reflections from the lower crust below the Danish–Norwegian Basin. The sections illustrate the variation in Moho-depth from the thick crust in the Ringkøbing–Fyn High to the thin crust in the Danish–Norwegian basin. Abbreviations: Pi: the first arrival P-wave which at this offset interval has been propagating through the lower crust, and PmP: the P-wave reflection from the Moho.

PmP reflections are absent for shot points 3 and 4 along the main profile. It shows a very weak PmP reflection in the central part of the section, corresponding to reflections from beneath the main profile, whereas there is substantial amplitude of the PmP reflection at both ends of the section. The width of the interval with weak or absent PmP reflections is about 45 km wide in the fan section, which corresponds to an approximately 22 km wide reflection free zone at the Moho level (at the mid-point between shot and receiver). This gives an indication for the possible dimensions of the zone of suggested feeder channels. The section indicates substantial lower crustal reflectivity at the northern end of the profile underneath the Danish–Norwegian basin, where the onset of the PmP reflection is uncertain due to the strong reverberative reflection character of the signals. The fan section further shows that, as expected, the Moho is deep in the Ringkøbing–Fyn High (more than 0.5 s later than at the main profile) to the south of the main profile.

The data from the eastern arc was recorded close to shot point 4 along the main profile, corresponding to reflections from an interval with strong PmP reflections along the main profile. Similar high-amplitude PmP reflections are observed in the fan recordings. The main finding from this fan profile is the delineation of the Moho slope from the thick crust underneath the Ringkøbing–Fyn High to the thin crust below the Norwegian–Danish Basin where, however, the exact time of the PmP may be masked by strong lower crustal reflectivity as in the western fan profile. Depending on the extent of the lower crustal reflectivity, the Moho, as recorded along both fan profiles, may be slightly shallower below the main profile (i.e. below the deep batholith) than below the general basin further to the north.

6. Discussion

The ESTRID refraction profile is located along the strike direction of the Silkeborg Gravity High. The data demonstrates the occurrence of high seismic velocity below a depth of 10–12 km over a horizontal interval of 75 km and a depth of ca. 16 km further along the strike of the anomaly. The high velocity of the high velocity body is larger than the value of 6.5 km/s in the tomographic velocity model because of averaging and smearing effects. Thus, we estimate that the true velocity is substantially larger, possibly up to 6.8 km/s at the top of the high velocity layer. The tomographic model shows velocities as large as 7.0 km/s at a depth of 24 km, which likewise indicates that true velocities are substantially larger than 7.0 km/s. This is unusual in the southern Scandinavian region where the velocity of the lowest crust rarely reaches 7.0 km/s, and, thus, this observation provides strong evidence for the presence of seismically anomalous crust to significant depths beneath the gravity high. We can at present not determine the degree of layering in the interpreted mafic intrusive body.

The EUGENO-S profile 2 crosses the ESTRID refraction profile at an oblique angle. The velocity model derived for this profile includes a high velocity body, which is up to 70 km wide (measured as the width of the region with velocity larger than 6.6 km/s) at 12 km depth, with a 45 km wide core of velocity above 6.9 km/s in the profile direction (Fig. 4). The angle of

this profile is about 45° to the strike direction of the body as determined from the gravity anomaly. Therefore, the true width of the body is of the order of 32 km for the core of the body and 50 km for the zone of elevated velocity. Determination of the velocity of the lowest crust is always subject to large uncertainty, but all the available data indicate that the high velocity continues to the Moho, as also interpreted in the EUGENO-S profile 2. This profile indicates that the Moho is 2–3 km shallower beneath the anomalous crustal body than below the surrounding basins. Integrated modelling of seismic and gravity data along EUGENO-S profile 2 has shown that the main gravity anomaly can be explained by the presence of an elongated body (Thybo and Schoenharting, 1991) with densities as predicted from the seismic velocities from laboratory measurements (Woollard, 1959; Dortmann and Magid, 1968).

Based on the above estimates we find that the amount of magmatic material that was added to the crust in the area of the ESTRID profile may be of the order of 60,000–100,000 km^3. The residual gravity field after stripping off the effects of the sedimentary sequences, indicates that the body extends for another 100 km to the east and that it may extend further northward than the ESTRID profile for another 100 km (Thybo and Schoenharting, 1991; Zhou and Thybo, 1996). Depending on the total thickness of the batholith in these zones, the total volume of magmatic rocks in the crust may be up to 300,000 km^3. Gravity highs of similar lateral extent and amplitude to the Silkeborg Gravity High are observed in the eastern part of the region at Scania and at the Oslo–Skagerrak Graben system. If these represent similar large quantities of magmatic rocks in the crystalline crust, the total volume could be up to 1 M km^3, which intruded into the crust over an area of 45,000 km^2. The accompanying heating of the lithosphere has been substantial, probably enough that the subsequent cooling may have initiated the subsidence of the regional basins (Sorensen, 1986; Vejbaek, 1989).

Seismic interpretation of the EUGENO-S profile 2 data identified a thin layer (a waveguide) with a velocity of ca. 6.25 km/s at a depth around 7 km along the central part of the profile (Fig. 4). A calculated residual gravity anomaly and the local magnetic intensity has been explained by this shallow body, which has large density and magnetic susceptibility compared to the surrounding sedimentary sequences, as well as strong, reversely oriented remanent magnetization. This waveguide has, so far, not been confirmed by the ESTRID data. It is stratigraphically situated at a level around the top of the Palaeozoic strata, and may be equivalent to late Carboniferous to early Permian volcanic rocks, which are commonly found throughout the region (Thybo and Schoenharting, 1991). Much of this period (the Kiaman period in the Permian) had a characteristic reverse polarity of the magnetic field and modelling has shown that the remanent magnetization of this layer is reverse. These findings indicate that the upper body represents a volcanic layer of late Carboniferous to early Permian age like most of the volcanic rocks in the region (e.g. Frost et al., 1981). The deep and larger crustal body may in this context be interpreted as a batholith which was emplaced during transtensional movement on the Vinding Fracture Zone, as indicated by its elongated shape. The large velocity and density of the former magma chamber indicates that it could have supplied the volcanic material that erupted close to the surface to form the present high velocity layer in the sedimentary sequence.

It has recently been suggested that the age of the magmatic feature at the Silkeborg Gravity High could possibly be Proterozoic instead of late Palaeozoic (Olesen et al., 2004). We find this idea intriguing, but for several reasons also unlikely: (1) the associated volcanic material is stratigraphically situated close to the base of the Zechstein (Permian) salt deposits, which shows that they must be of Palaeozoic age, (2) the Permian included a long period with a magnetic reversal, the Kiaman period, (3) the widespread volcanic rocks of late Carboniferous to early Permian age indicates a likely similar age of the observed volcanic horizon, (4) the occurrence of an intracrustal magmatic body might be expected to have caused volcanic eruptions of similar age. It cannot be totally excluded that a part of the main magmatic body may be older than the Carboniferous–Permian, but a large part of the magmatic rocks must have been emplaced at the time of the volcanic eruptions.

The ESTRID data show that the crust along the profile is non-reflective below the top of the basement. Reflections from the interior of the crystalline crust have not been observed in any of the ESTRID seismic sections, which all were acquired along the strike of the batholith. However, the two fan profiles indicate that the lower crust outside the magmatic body may be reflective, in particular below the Danish–Norwegian Basin. This is also observed in other profiles from the area, including the EUGENO-S profiles 1, 2, 3 and 5 (EUGENO-S Working Group, 1988; Thybo et al., 1990; Thybo and Schoenharting, 1991; Thybo et al., 1998) and the MONA LISA profiles from the North Sea (MONA-LISA-Working-Group, 1997; Abramovitz and Thybo, 1998; Abramovitz et al., 1999). These findings show that there is no large-scale internal layering in the

magmatic body, at least not over the wide frequency band that was used for the ESTRID project. This further indicates that the intrusion may have taken place during only a few major pulses of magma supply, which were followed by slow cooling such that abrupt transitions in rock types did not develop inside the body. It also appears unlikely that the intrusions were emplaced in the form of isolated sills as interpreted in the Kenya Rift Zone Rift (Birt et al., 1997; Thybo et al., 2000), because such structure would produce sharp contrasts in acoustic impedance. This observation may have large implications for future subsidence modelling of the Danish–Norwegian Basin with the perspective of identification of new hydrocarbon plays. There is little doubt about the hydrocarbon potential of the Palaeozoic sedimentary rocks, depending on the heating and subsidence history of the relevant strata.

7. Conclusions

The ESTRID refraction profile has provided evidence for the presence of an elongated body with characteristic high seismic velocity and density in the crystalline crust of the Danish–Norwegian Basin below a depth of 10–12 km. Identification of a thin layer of high seismic velocity, density and magnetic susceptibility, as well as strong, reverse remanent magnetization, indicates the presence of volcanic rocks in Carboniferous to Permian sedimentary sequences. We therefore interpret the intracrustal body as a batholith of Carboniferous–Permian age. The estimated volume of magmatic material that has been added to the crust near the ESTRID profile may be of the order of 60–300,000 km^3, depending on the lateral extent of the body. New reflection seismic data has been acquired in September 2005 in order to image the internal structure of the batholith. The intention of this effort is to provide more precise estimates of the amount of magma that intruded into the crust and its internal structure, which will allow well constrained modelling of the subsequent subsidence processes.

Acknowledgments

The authors acknowledge the enthusiastic participation of 40 B.Sc., M.Sc. and Ph.D. students from the Universities of Copenhagen and Aarhus in the acquisition of the ESTRID seismic data. The project benefited from the general technical expertise by electrical engineer Peer Jørgensen (Copenhagen) and the shooting expertise by professor emeritus Kayan Aric, Vienna, and Captain T. Pedersen from the Royal Guard Regiment (Skive). The seismic instruments were provided by the University of Texas at El Paso through the IRIS/Passcal facility that is supported by the National Science Foundation and the University of Copenhagen. Project ESTRID is carried out in the Centre for Integrated Geophysical Research, which is funded by the Danish Natural Science Research Council and the Carlsberg Foundation.

References

Abramovitz, T., Thybo, H., 1998. Seismic structure across the Caledonian deformation front along MONA LISA Profile 1 in the southeastern North Sea. Tectonophysics 288 (1–4), 153–176.

Abramovitz, T., Thybo, H., 2000. Seismic images of Caledonian, lithosphere-scale collision structures in the southeastern North Sea along MONA LISA Profile 2. Tectonophysics 317 (1–2), 27–54.

Abramovitz, T., Landes, M., Thybo, H., Jacob, A.W.B., Prodehl, C., 1999. Crustal velocity structure across the Tornquist and Iapetus suture zones; a comparison based on MONA LISA and VARNET data. Tectonophysics 314 (1–3), 69–82.

Achauer, U., Masson, F., 2002. Seismic tomography of continental rifts revisited; from relative to absolute heterogeneities. Tectonophysics 358, 17–37.

Bastow, I., Stuart, G., Kendall, J.M., Ebinger, C., 2005. Upper-mantle seismic structure in a region of incipient continental breakup: Northern Ethiopian Rift. Geophysical J. Int. 162, 479–493.

Benek, R., et al., 1996. Permo-Carboniferous magmatism of the Northeast German Basin. Tectonophysics 266, 379–404.

Berndt, C., Skogly, O.P., Planke, S., Eldholm, O., Mjelde, R., 2000. High-velocity breakup-related sills in the Voring Basin, off Norway. Journal of Geophysical Research 105 (12), 28443–28454.

Berthelsen, A., 1992. Mobile Europe. In: Blundell, D.J., Mueller, St., Freeman, R. (Eds.), A Continent Revealed, The European Geotraverse Project. Cambridge University Press, pp. 11–32.

Birt, C.S., et al., 1997. The influence of pre-existing structures on the evolution of the southern Kenya Rift valley; evidence from seismic and gravity studies. Tectonophysics 278 (1–4), 211–242.

Cartwright, J., 1990. The structural evolution of the Ringkobing–Fyn High. In: Blundell, D.J., Gibbs, A.D. (Eds.), Tectonic Evolution of the North Sea Rifts. Publication (International Lithosphere Program). Oxford University Press, New York, NY, International, pp. 200–216.

Collier, J.S., Buhl, P., Torne, M., Watts, A.B., 1994. Moho and lower crustal reflectivity beneath a young rift basin; results from a two-ship, wide-aperture seismic-reflection experiment in the Valencia Trough (western Mediterranean). Geophysical Journal International 118 (1), 159–180.

Dikkers, A.J., 1977. Sketch of a possible lineament pattern in Northwest Europe. Geologie en Mijnbouw 56, 275–285.

Dortmann, N.B., Magid, M.Sh., 1968. Elastic wave velocity in crystalline rocks and its dependence on moisture content. Sovetskaya Geologiya 5, 123–129.

EUGENO-S Working Group, 1988. Crustal structure and tectonic evolution of the transition between the Baltic Shield and the North German Caledonides (the EUGENO-S Project). Tectonophysics 150, 253–348.

Fowler, S.R., White, R.S., Spence, G.D., Westbrook, G.K., 1989. The Hatton Bank continental margin; II, Deep structure from two-ship expanding spread seismic profiles. Geophysical Journal of the Royal Astronomical Society 96 (2), 295–309.

Frost, R.T.C., Fitch, F.J., Miller, J.A., 1981. The age and nature of the crystalline basement of the North Sea Basin. In: Illing, L.V., Hobson, G.D. (Eds.), Petroleum Geology of the Continental Shelf of North-West Europe; Proceedings of the Second Conference. Heyden and Son, London, United Kingdom, pp. 43–57.

Fujita, K., Sleep, N.H., 1991. A re-examination of the seismicity of Michigan. Tectonophysics 186, 75–106.

Gao, S., et al., 1994. Asymmetric upwarp of the asthenosphere beneath the Baikal rift zone, Siberia. Journal of Geophysical Research, B, Solid Earth and Planets 99 (8), 15,319–15,330.

Hay, D.E., Wendlandt, R.F., Keller, G.R., 1995. The origin of Kenya rift Plateau-type flood phonolites: Integrated petrologic and geophysical constraints on the evolution of the crust and upper mantle beneath the Kenya rift. Journal of Geophysical Research 100, 10,549–10,557.

Hole, J.A., 1992. Nonlinear high-resolution three-dimensional seismic travel time tomography. Journal of Geophysical Research, B, Solid Earth and Planets 97 (5), 6553–6562.

Johnston, A.C., 1987. Air blast recognition and location using regional seismographic networks. Bulletin of the Seismological Society of America 77, 1446–1456.

Keller, G.R., et al., 1994. The East African rift system in the light of KRISP 90, in Crustal and Upper Mantle Structure of the Kenya Rift. Tectonophysics 236, 465–483.

Kendall, J.M., Stuart, G., Ebinger, C., Bastow, I., Keir, D., 2005. Magma assisted rifting in Ethiopia. Nature 433, 146–148.

Lassen, A., Thybo, H., 2004. Sveconorwegian basement structures and their relation to the formation of the Danish Basin, examples from the Kattegat area. Tectonics 23. doi:10.1029/2003TC001499.

Lassen, A., Thybo, H., submitted for publication. Neoproterozoic and Palaeozoic evolution of SW Scandinavia based on integrated reflection seismic interpretation. Precambrian Research.

Mackenzie, G., Thybo, H., Maguire, P., 2005. Crustal velocity structure across the Main Ethiopian Rift: results from 2-dimensional wide angle seismic modelling. Geophysical J. Int. 162, 994–1006.

Maguire, P.K.H., Swain, C.J., Masotti, R., Khan, M.A., 1994. A crustal and uppermost mantle cross-sectional model of the Kenya Rift derived from seismic and gravity data. Tectonophysics 236, 217–249.

McKenzie, D., 1978. Some remarks on the development of sedimentary basins. Earth and Planetary Science Letters 40 (1), 25–32.

MONA-LISA-Working-Group, 1997. MONA LISA; deep seismic investigations of the lithosphere in the southeastern North Sea. Tectonophysics 269 (1–2), 1–19.

Neumann, E.R., Olsen, K.H., Baldridge, W.S., Sundvoll, B., 1992. The Oslo Rift; a review. Tectonophysics 208 (1–3), 1–18.

Olesen, O., Smethurst, M.A., Torsvik, T., Bidstrup, T., 2004. Sveconorwegian igneous complexes beneath the Norwegian–Danish Basin. Tectonophysics 387, 105–130.

Petit, C., Koulakov, I., Deverchere, J., 1998. Velocity structure around the Baikal rift zone from teleseismic and local earthquake traveltimes and geodynamic implications. Tectonophysics 296 (1–2), 125–144.

Ro, H.E., Faleide, J.I., 1992. A stretching model for the Oslo Rift. In: Ziegler Peter, A. (Ed.), Geodynamics of Rifting; Volume I, Case History Studies on Rifts; Europe and Asia. Tectonophysics. Elsevier, Amsterdam, Netherlands, pp. 19–36.

Scheck, M., Thybo, H., Lassen, A., Abramovitz, T., Laigle, M., 2002. Basement structure in the Southern North Sea, offshore Denmark, based on seismic interpretation. Geological Society, London, Special Publication 201, 311–326.

Sorensen, K., 1986. Danish Basin subsidence by Triassic rifting on a lithosphere cooling background. Nature (London) 319 (6055), 660–663.

Thybo, H., 1997. Geophysical characteristics of the Tornquist fan area Northwest Trans-European suture zone; indication of Late Carboniferous to Early Permian dextral transtension. Geological Magazine 134, 597–606.

Thybo, H., 2001. Crustal structure along the EGT profile across the Tornquist Fan interpreted from seismic, gravity and magnetic data. Tectonophysics 334, 155–190.

Thybo, H., Schoenharting, G., 1991. Geophysical evidence for Early Permian igneous activity in a transtensional environment, Denmark. Tectonophysics 189 (1–4), 193–208.

Thybo, H., Kiørboe, L.L., Møller, C., Schönharting, G., Berthelsen, A., 1990. Geophysicial and tectonic modelling of EUGENO-S profiles. In: Freeman, R., Mueller, S. (Eds.), Proceedings of the VI Workshop on the European Geotraverse Project, Strasbourg, pp. 93–104.

Thybo, H., Perchuc, E., Gregersen, S., 1998. Interpretation in Statu Nascendi of seismic wide-angle reflections based on EUGENO-S data. Tectonophysics 289, 281–294.

Thybo, H., Maguire, P.K.H., Birt, C., Perchuc, E., 2000. Seismic reflectivity and magmatic underplating beneath the Kenya Rift. Geophysical Research Letters 27 (17), 2745–2748.

Vejbaek, O.V., 1989. Effects of asthenospheric heat flow in basin modelling exemplified with the Danish Basin. Earth and Planetary Science Letters 95 (1–2), 97–114.

Vejbaek, O.V., 1990. The Horn Graben, and its relationship to the Oslo Graben and the Danish Basin. Tectonophysics 178 (1), 29–49.

Vidale, J.E., 1988. Finite-difference calculation of travel times. Bulletin of the Seismological Society of America 78 (6), 2062–2076.

Woollard, G.P., 1959. Crustal structure from gravity and seismic measurements. Journal of Geophysical Research 64 (10), 1521–1544.

Zelt, C.A., Smith, R.B., 1992. Seismic traveltime inversion for 2-D crustal velocity structure. Geophysical Journal International 108, 16–34.

Zhou, S., Thybo, H., 1996. Calculation of residual gravity anomalies in northern Jutland, Denmark. First Break 14 (4), 129–134.

Ziegler, P.A., 1990. Geological Atlas of Western and Central Europe. The Hague: Shell Internationale Petroleum Maatschappij/Amsterdam: Elsevier. 239 pp.